VASCULATURE SEGMENTATION OF CT LIVER IMAGES USING GRAPH CUTS AND GRAPH-BASED ANALYSIS

Hanno Homann, Grace Vesom and J. Alison Noble

Department of Engineering Science, University of Oxford, Oxford, UK

ABSTRACT

Extracting hepatic vasculature from 3D imagery is important for diagnosis of liver disease and planning liver surgery. In this paper we propose to segment vessels from liver CT images using a 3D graph-cuts based method that utilizes probabilistic intensity information and surface smoothness as constraints. A semi-automatic graph-based technique is then employed to efficiently separate the hepatic vessel systems. The complete vascular analysis method has been evaluated on 6 liver CT datasets using manual segmentation as the reference and showing that the method is reasonable robust to parameter choice and gives results of similar accuracy to previous methods in a time-efficient manner.

Index Terms— vascular segmentation and analysis, graph cuts, liver analysis, oncology.

1. INTRODUCTION

In planning treatment for cancer in the liver, it is crucial to have exact knowledge of liver tumors and their 3D location relative to the liver vasculature. There are increasingly different options for treating liver cancers, ranging from surgery, radiofrequency ablation, chemotherapy and radiotherapyCT and MR images are used in disease diagnosis and therapy assessment. These are used to look at the liver volume, to characterize masses as well as to visualize the vasculature. Liver images are surprisingly difficult to analyze due to the variable shape of a natural liver, many organs/tissues touching the surround of the liver, and the relatively low contrast of vessels. Indeed a workshop at MICCAI 2007 was dedicated to evaluating state-of-the-art methods of liver CT volume segmentation [1].

Segmentation of the liver vascular system, including separation of the portal vein, hepatic vein, and hepatic artery systems is important clinically, to precisely localize liver cancer, metastases, and other lesions; to approximate liver segments (by say the Couinaud segment system) and show areas of blood supply, and to provide a patient-specific 3D visualization of key liver structures for treatment planning. Contrast-enhanced CT, with phase-gating to enhance different components of the liver anatomy, is typically used for vessel visualization, because it has superior spatial resolution to MRA.

There is an extensive literature on vasculature segmentation for MRA and CT data, particularly for applications in neurology and cardiology. Some authors have treated vessel segmentation as a tracking problem, where vessels are iteratively tracked constrained using information on the centerlines, and local features [2,3]. This class of approach is fast, but requires special routines to handle branch points and some user-interaction to initialize. Level-sets methods [4,5] have proved popular for MRA-segmentation but require good initialization and typically use speed functions which implicitly assume good contrast data which is not the case for liver CT images. Intensity-threshold-based methods have shown some promise for liver CT images. Soler et al [6] use a global threshold histogram-based approach followed by a number of post-processing steps but did not present an evaluation of their method. Selle et al [7] define an "optimal" intensity threshold using region-growing, but their method appears to only be suitable for large vessels.

In this paper we propose to use the graph cuts framework [8] for vascular segmentation which to our knowledge has not been investigated before in this context. The graph cuts method is a relatively new segmentation technique; the basic idea is to represent the image as a graph in which every voxel corresponds to a node. Depending on a cost function, the graph is separated (cut) into two subsets. The attractive properties of the method for vascular segmentation are that it (1) computes a global optimum of a cost function in low-order time; (2) requires no geometric initialization; and, (3) allows for incorporation of region information and boundary constraints in a natural way.

2. ALGORITHM

2.1. Overview

The algorithm that has been developed takes as input a liver CT image and produces a delineation of the different vessel subsystems (see Figure 5). Figure 1 shows a flowchart of the key steps. The method starts by cropping the volume of interest (i.e. the liver) and performing anisotropic diffusion as a pre-segmentation step. A graph cuts segmentation method (sect 2.2) is employed to detect vessels, and then the vasculature sub-trees are identified using skeletonization followed by a novel graph-based analysis (sect 2.3).

2.2. Segmentation using Graph Cuts

Due to space constraints, we assume some familiarity with the concept of graph cuts [8]. Briefly the idea is to form a weighted graph $G = (V \cup \{s,t\}, E)$ where the node set $V \cup \{s,t\}$ contains all voxels $v \in V$ and two additional terminal nodes, the source *s* and sink *t*.

For image segmentation, the edge-set *E* consists of *n-links* which connect neighboring voxels and *t-links* that connect all voxels *v* to *s* and *t*. The goal is to find the optimal cut of a cost function defined as the sum of the weights of the cut edges. The labeling vector $\underline{L}$ marks each voxel p in the image *V* as object *O* or background *B*. The link between a pair of neighboring voxels $\{p,q\}$ in a neighborhood *N* is cut if $L_p \neq L_q$. Then the cost $|C|$ is defined as,

$$|C|(\underline{L}) = \sum_{\{p,q\} \in N} B_{p,q} \cdot \delta(L_p, L_q) + \sum_{p \in V} R_p(L_p). \qquad (1)$$

Here the n-weights (term 1 in eqn 1) are determined by [8]

$$B_{p,q} = \lambda_B \cdot \exp\left(-\frac{\Delta I^2}{2\sigma^2}\right), \qquad (2)$$

where $\Delta I = I_p - I_q$, and λ_B, σ are parameters and $\delta(L_p, L_q) = 1 \; if \; L_p \neq L_q$ or 0 otherwise. The t-weights (term 2 in eqn 1) are determined as

$$R_p(X) = \lambda_L \cdot P(I = I_p \mid X), \qquad (3)$$

where P(I|X) is the probability of intensity *I* being a member of class *X*, *X=O* or *B,* and λ_L is a third parameter.

The min-cost cut defined in Eqn. 1 can be solved using any max-flow algorithm. We use an enhanced version of the augmenting paths algorithm which is publically available [9] and solves the max-flow problem in low-order polynomial time.

We determine the intensity distribution P(I|O) by interactively marking some vessels in a single representative 2D slice as suggested in [8]. Since the portion of vessels in the image is usually very small, we can assume that P(I|B)=P(I). A bin width of 5HU was chosen in the implementation which we have found gives a sufficiently smooth probability function. A typical intensity histogram for a low contrast dataset is shown in Fig 2.

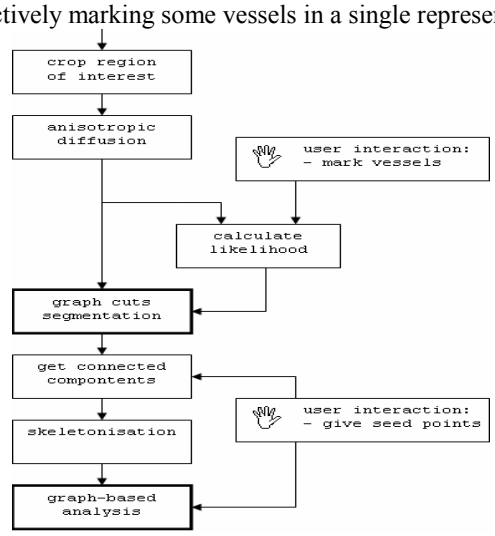

Figure 1: Flowchart of vascular analysis algorithm.

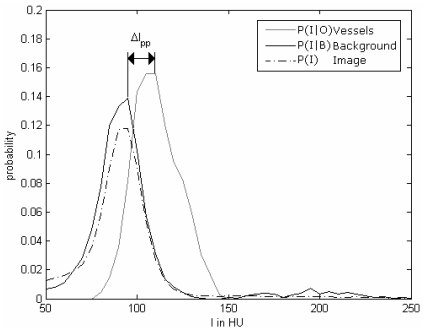

Figure 2: Intensity distribution for low contrast vessels.

2.3 Vasculature Geometry Graph Construction

Since no shape prior is included to this point, the vessel segmentation from the graph cuts algorithm tends to leak into background structures (ribcage, tumors, kidneys) if they are of similar intensity. Furthermore, the portal and the hepatic venous system are often linked via pseudo-connections. To improve the segmentation results, we use the following graph-based analysis to incorporate geometric *a priori* knowledge. First a 3D skeletonization algorithm is applied [10] – this particular algorithm uses 26-neighborhood connectivity of the object. The 3D skeleton is then used to create a geometric graph G (note: though used in sect 2.2 in another context, we prefer to use this symbol G again here as it is the one used most often in related work). In this case, the edges and nodes of G represent the branching points and adjacent vessel segments respectively. The generation of G is realized as follows:

1. All skeleton voxels with more than 2 neighbors are marked branching points and added as nodes to G.
2. All skeleton voxels with only 1 neighbor are end points.
3. All skeleton contours are traced until the next branching/end point and added to G as undirected edges.

The Boost Graph Library (www.boost.org/libs/graph) is used for handling the graph. Additional information stored is the estimated bifurcation angle α for each node (branch point) and the averaged radius r for each edge.

Our *a priori* knowledge of the hepatic vessel systems is that (1) they are tree-shaped; (2) do not form loops, (3) the thickness of vessels reduces in the flow direction, and (4) there are no obtuse angles between vessels at branch points [6]. We can use this information to design a deterministic classifier to mark each edge as part of the portal or hepatic venous system or background (non-vascular). Classification is achieved using the two algorithms given below.

If only one vessel system is contrast enhanced, only the removal of the background structures is required (Alg 1): One or more major branches are selected by the user. Each adjacent branch is added to the vessel tree, if its radius is smaller than the radius of the first branch and the bifurcation angle is reasonably large. A hysteresis threshold $\Delta r_{\max}$ for the radius of is used. Alg 1 iterates for all newly added branches and terminates if $r_{\min}$ is reached.

If more than one vessel system is present, we use Alg 2 to separate them at the smallest connecting branch: This algorithm calls Alg 1 to add the larger branches to both vessel systems first. The minimal radius $r_{\min}$ is the reduced and Alg 1 is called again, so that both vessel trees continuously grow more detailed. If at any step a branch is claimed by both trees, it cannot be classified and is removed from the graph.

Algorithm 1 (Removal of non-vascular structures)

FOR all edges adjacent to the vessel tree
  IF $r_{\min} \le r \le r_{prev} + \Delta r_{\max}$ AND $\alpha \ge \alpha_{\min}$
    THEN label adjacent edge as part of vessel tree
    AND examine adjacent edges beyond current one
  END IF
END FOR

Algorithm 2 (Separation of vessel systems)

FOR $r_{\min}$ =15mm decremented to 2mm, stepsize 1mm
  CALL Algorithm 1 for portal vein and current $r_{\min}$
  CALL Algorithm 1 for hepatic vein and current $r_{\min}$
  FOR edges labeled in both trees
    REMOVE edge
  END FOR
END FOR

3. EXPERIMENTS AND RESULTS

3.1 Datasets

Six datasets were used, 3 from the Oxford John Radcliffe Hospital NHS Trust, and 3 from the MICCAI07 workshop database [1]. Relevant details are summarized in Table 1 (Rows 1-3) together with a measure of the difficulty in automated segmentation (Row 4), defined as the difference in peaks between the vessel and background distributions (see Fig 2). Note that the MICCAI datasets were superior to the Oxford datasets in this respect. Manual segmentation by one of the authors (HH) was used as the reference against which to evaluate algorithm performance. Performance is reported using the Dice Similarity Coefficient (DSC).

3.2 Graph cuts sensitivity to choice of parameters

Our segmentation algorithm has 3 parameters, $\lambda_B, \lambda_L, \sigma$. Experiments were done to determine the parameter ranges in which the best algorithm results could be obtained.

Parameter λ_L : was evaluated assuming $\lambda_B = \sigma = 0$ i.e. a purely voxel-based MLE, based on the user-selected intensity distribution. The DSC was calculated over a parameter range $\lambda_L \in [0,100]$ in increments of 5. Results are plotted in Fig 3(a) which shows that for $\lambda_L > 30$, the DSC value is approximately constant, below this the result is unstable, possibly due to rounding errors in the minimum cost cut calculation. Note that OX2 and OX3 have low DSC values due to the presence of a lesion which is of similar intensity to that of vessels. Both datasets were excluded from further parameter setting validation.

Parameter σ : is a measure of image noise. Homogeneous regions of liver parenchyma were selected, and the std dev. of a Gaussian fitted to the histograms estimated, see Table 1 (Row 5). This shows that this varies from dataset

	OX1	OX2	OX3	MIC1	MIC2	MIC3
1) Resolution (x,y,z) in mm	0.703, 0.703, 5.0	0.626, 0.625, 5.0	0.684, 0.684, 2.5	0.742, 0.742, 1.5	0.629, 0.8629, 3.0	0.760, 0.760, 3.0
2) Enhanced vessels	PV, HV	HV	PV, HV	PV	PV, HV	PV,HV
3) Contrast agent	n.s.	100 ml NIO 300	100 ml NIO 300	n.s.	n.s.	n.s.
4) Vessel contrast	30 HU	15 HU	40 HU	75 HU	70 HU	105 HU
5) Image noise	4.1 HU	3.5 HU	6.4 HU	10.2 HU	6.3 HU	5.5 HU
6) DSC (adjusted DSC)	0.77	0.61 (0.63)	0.44 (0.70)	0.59	0.83	0.72
7) PV edges	80	-	366	1117	562	200
8) HV edges	84	147	92	-	275	121
9) UC edges	2	-	2	-	16	1
10) Total length PV	0.44 mm	-	1.93 mm	3.74 mm	3.22 mm	1.07 mm
11) Total length HV	0.60 mm	1.36 mm	0.41 mm	-	1.70 mm	0.88 mm

Table 1: Data analysis of the Oxford (OX) and MICCAI (MIC) datasets : Rows 1-3 details of acquisition, Row 4 estimated vessel contrast (see sect. 3.1), Row 5 estimated noise (sect 3.2), Row 6 DSC value for best parameter settings (sect 3.2), Rows 7-9 number of edges in final vessel system, Rows 10-11 accumulated length from graph-based analysis.
PV=portal vein, HV=hepatic vein, UC=unconnected, n.s.=not specified.

to dataset and hence can not be assumed a constant. We therefore empirically investigated varying σ keeping $\lambda_L = 40, \lambda_B = 15$ (see Fig 3(b)). The conclusion is that $\sigma \in [2,6]$ gives acceptable results.

Parameter λ_B: Using $\sigma = 2, \lambda_L = 100, \lambda_B$ was varied in [0,50] but this had little effect on the DSC value. This is as expected as λ_B effects vessel smoothness (Fig 4) and thus only changes vessel labels on the vessel boundary which does not change the DSC value significantly.

Based on the above analysis we used $\sigma = 2, \lambda_L = 35, \lambda_B = 15$, in subsequent analysis for all datasets. The DSC values for these parameter settings for the 6 datasets are shown in Table 1 (Row 6). Manual removal of the lesions from the segmentations of OX2 and OX3 could improve the DSC in both cases.

When examined visually, both the vessel surfaces and skeleton lines were clean and smooth (Fig. 5, left).

3.3 Graph-based analysis

Results of applying the complete graph-based analysis for a representative dataset (MIC2) are shown in Fig. 5 (right). Note that graph-analysis algorithm 1 eliminates extra-hepatic structures such as the aorta and kidneys. Most intra-hepatic lesions are detected and removed. The algorithm classifies all major vessels correctly in our 6 datasets.

The total accumulated length is reported in Table 1 (Rows 10-11) and well as the number of edges in the portal and hepatic venous systems as well as unclassified edges Rows (7-9). These values are as good if not better than those reported in [7].

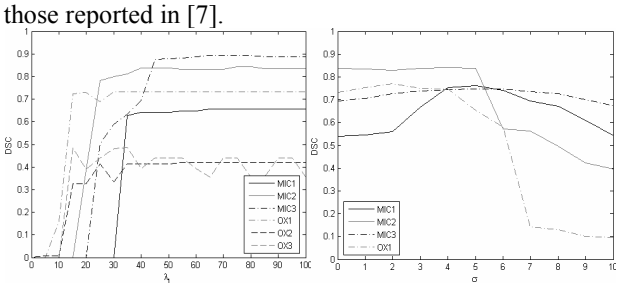

Fig 3: (a) evaluation of λ_L, and (b) evaluation of σ in graph cut segmentation method.

Fig 4: Effect of λ_B on segmentation (left) $\lambda_B = 0$ and (right) $\lambda_B = 30$.

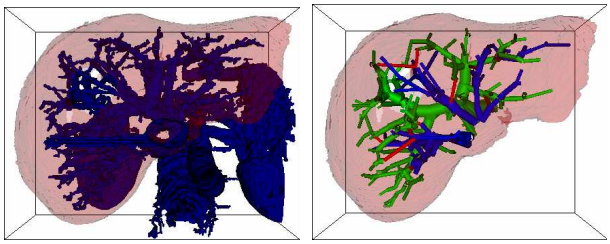

Fig 5: MIC2 dataset: (left) Segmentation and (right) graph representation with hepatic veins (dark-blue), portal veins (light-green), and vessels not classified (red).

4. DISCUSSION AND CONCLUSION

We have presented a novel method for analysis of complex vessel systems from 3D liver CT images. Our approach uses probabilistic intensity information and surface smoothness as constraints. We also presented an algorithm to separate the different hepatic vasculatures.

We have evaluated the segmentation step on 6 datasets, and found the algorithm to be robust in a certain parameter range. The computation time for segmentation and analysis on a standard PC (1.6GHz CPU, 512MB RAM, Windows XP) is reasonable although it varied considerably dependent on the complexity of the resolved object rather than image size. Future work includes combining this work with a liver shape segmentation and investigating the application of the methodology in treatment planning.

ACKNOWLEDGMENTS

We thank the organizers of the MICCAI workshop "3D Segmentation in the Clinic - A Grand Challenge", Tobias Heimann, Martin Styner, and Bram van Ginneken, for providing the datasets used in this work.

5. REFERENCES

[1] 3D segmentation in the clinic: a grand challenge, T Heimann, N Styner, B van Ginneken (Eds), pp 7-15, 2007.

[2] Aylward S, Bullitt E, IEEE TMI 21:2:61-75, 2002.

[3] Florin C et al, Particle filters, a quasi-monte carlo solution for segmentation of coronaries, MICCAI2005 pp 246-253, 2005.

[4] Lorigo LM, et al, CURVES: curve evolution for vessel segmentation, MedIA, 5:3:195-206, 2001.

[5] Yan P, Kassim AA, Segmentation of volumetric MRA images using capillary active contour, MedIA, 10:317-329,2006.

[6] Soler L, et al, Fully automatic anatomical, pathological and functional segmentation from CT scans for hepatic surgery, Comp. Aid. Surgery 6:131-142, 2001.

[7] Selle D, et al, Analysis of vasculature for liver surgical planning, IEEE TMI 21:11:1344-1357, 2002.

[8] Boykov Y, Jolly MP, Interactive Graph Cuts for Optimal Boundary & Region Segmentation of Objects in N-D Images, ICCV 1:105-112, 2001.

[9] Kolmogorov V, An implementation of the maxflow algorithm, www.adastral.ucl.ac.uk/~vladkolm/software.html

[10] Lee TC et al, Building skeleton models via 3-D medical surface/axis thinning algorithms, CVGIP 56:6:462-478, 1994.